Effect of pH Conditions on Actual and Apparent Fluoride Adsorption by Biochar in Aqueous Phase

Taek-Keun Oh · Bongsu Choi · Yoshiyuki Shinogi · Jiro Chikushi

Abstract Biochar is a carbon-rich product derived from biomass through pyrolysis. Fluoride adsorption potential of the biochar derived from orange peel (OP) and water treatment sludge (WS) at different pyrolytic temperatures (400, 600, and 700 °C) was investigated in a batch mode as a function of pH. With respect to adsorption, two types were considered, i.e., actual and apparent adsorption where fluoride combined with metal complexes in solution were counted and not counted, respectively. The highest actual fluoride adsorption was observed in the pH range of 2.0 to 3.9 for OP biochar and 5.1 to 6.2 for WS biochar, respectively. For the WS biochar, apparent fluoride adsorption showed nearly 100 % in the pH range of 2.0 to 4.5, and then the adsorption capacity diminished drastically as the pH increased from 5.0 to 10.0. There was no significant difference between apparent and actual fluoride adsorption for OP biochar. In the Fourier-transform infrared spectroscopic analysis of WS biochar, a strong and sharp band was observed at around 2,364 cm^{-1} after adsorption of fluoride. Elemental content analysis by the energy-dispersive X-ray method revealed that the fluorine content was higher at pH 6.0 than at pH 3.0 and 9.0 as the results of actual fluoride adsorption. From these results, we may conclude that the biochar derived from OP and WS can be reused as an economical and effective adsorbent for fluoride removal in acidic aqueous phase.

Keywords Biochar · Fluoride · Adsorption · Orange peel · Water treatment sludge

Taek-Keun Oh and Bongsu Choi contributed equally to this work and should be considered co-first authors

T.-K. Oh (✉) · J. Chikushi
Biotron Application Center, Kyushu University,
Hakozaki 6-10-1, Higashi-ku,
Fukuoka City 812-8581, Japan
e-mail: otgwins@agr.kyushu-u.ac.jp

B. Choi
National Ecological Institute Planning Office,
Gwacheon, Gyeonggi 427-800, South Korea

Y. Shinogi
Science for Bioproduction Environment,
Faculty of Agriculture, Kyushu University,
Hakozaki 6-10-1, Higashi-ku,
Fukuoka City 812-8581, Japan

1 Introduction

Fluoride ion at low concentrations of 1.0–1.5 mg l^{-1} is essential and beneficial for human health, especially in promoting the development of strong bones and the formation of dental enamel (Rao and Karthikeyan 2011). The World Health Organization (WHO) proposed that the maximum concentration of fluoride in drinking water should not exceed 1.5 mg l^{-1} (WHO 2006) because chronic ingestion above this level might cause serious diseases such as dental and skeletal fluorosis (Groves 2001; Harrison 2005). However,

high concentration of the fluoride in water sources was reported in many areas around the world where the fluoride concentration is 0.01–3 mg l^{-1} in freshwater and 1.0–35 mg l^{-1} in groundwater (Oh et al. 2009; WHO 1994). For example, an investigation in Boeun, South Korea showed that about 23 % of total public water supply wells have fluoride levels exceeding the drinking water allowance in South Korea (1.5 mg l^{-1}) and the maximum fluoride concentration is 3.9 mg l^{-1} (Chae et al. 2008). Dental fluorosis was also observed among children in Aichi Prefecture, Japan, in 1970s, following the unintentional supply of drinking water containing up to 7.8 mg l^{-1} fluoride since 1960 (Ishii and Suckling 1991). Actually, around 200 million people, from over 25 countries, are under the dreadful fate of the fluorosis (Ayoob and Gupta 2006).

Extensive researches have been tried to remove excessive fluoride from water reservoirs by many methods such as adsorption, precipitation, electrodialysis, ion exchange, and reverse osmosis. Among many methods, the adsorption is considered as one of the most widely used and effective techniques for fluoride removal in drinking water (Meenakshi and Maheshwari 2006) because of its high efficiency and easy handling. Recent research has been focused upon the development of socially acceptable and economical adsorbents for the fluoride removal. Porous carbons, such as activated carbons and carbon nanotubes, are most common adsorbents for the fluoride adsorption because they have large surface area and continuous porosity (Tchomgui-Kamga et al. 2010). However, despite their effectiveness, their widespread use is restricted due to high associated costs (Chen and Chen 2009). It is therefore necessary and imperative to investigate the relatively inexpensive but effective and environmental adsorbent for the fluoride removal from contaminated water system.

Biochar is the carbon-enriched and porous material produced from variety of biomass through pyrolysis process. The biochar is similar to activated carbon, which is known as an effective adsorbent for the fluoride removal from aqueous solutions (Zheng et al. 2010). The various functional groups on surface of the biochar may affect the adsorption through the property of surface charge. The charge definitely depends upon the pH of solution (Lehmann and Joseph 2009). Although the biochar would potentially have the adsorption capacity of fluoride, there

is little information on the adsorption of fluoride by the biochar.

In this study, we investigated the possibility of biochar as adsorbents for removing aqueous fluoride by considering the conditions of pH. As the orange peel (OP) and water treatment sludge (WS) are becoming the environmental problem, such as management and disposal as agricultural and industrial biomass, we focused on the biochar derived from OP and WS at different pyrolytic temperatures. These biochars seem to have potential of adsorbent because they look like an activated carbon. We can also deduce that they typically contain various interesting functional groups, such as carboxyl and hydroxyl, hydrous oxides, and rugged surfaces, influencing the adsorption.

2 Materials and Methods

2.1 Biochar Preparation

Two different types of biomass, i.e., OP and WS, were used as raw feedstock for the biochar preparation. The orange fruits were obtained in a local fruit market, and their peels were stripped off with a paring knife. For easy storage and management, the OP was washed with distilled water three times to remove dusts and then was cut into small pieces of an average area of 1 cm^2. We also collected the WS from a drinking-water treatment plants located in Tatara, Fukuoka Prefecture, Japan, in which WS polyaluminum chloride (PAC) is used as coagulant. These collected OP and WS were air-dried at room temperature for 3 days and subsequently oven-dried overnight at 75±5 °C. The oven-dried feedstock were used for biochar production via pyrolysis at various temperatures under oxygen-limited conditions. The biochar preparation was done according to the method described by Oh et al. (2012). Initially, the different feedstock were placed into a stainless steel dish in a muffle furnace, covered with fitting lid to restrict the access of air during carbonization and then pyrolyzed for 2 h under different temperatures of 400, 600, and 700 °C. The resulting biochar were crushed and sieved into less than 2-mm size and stored in air-tight containers for the following experiments. For comparison, the oven-dried feedstock passed through 2-mm size was also used. In the following, the prepared biochar are denoted by OPB$_{xxx}$ or WSB$_{xxx}$, where OPB and WSB represent

the OP biochar and WS biochar, respectively, and *xxx* refers to the pyrolying temperature in °C.

2.2 Characterization of Samples

The pH of feedstock and biochar were measured in a 1:10 (samples:distilled water) using a pH meter (F-21, HORIBA). Carbon (C), hydrogen (H), and nitrogen (N) compositions were analyzed using elemental analyzer (Yanaco CHN Corder MT-5). Oxygen (O) content was determined from the mass balance of these compositions. Ash content was measured by heating the samples at 900 °C for 4 h and expressed as a percentage by mass. To determine the pH at the point of zero charge (pH_{pzc}), we prepared solution of 0.1 g of sample into 250 ml glass beaker containing 50 ml of 0.01 M NaCl solutions. The solutions were initially adjusted to have pH of 2.0, 4.0, 6.0, 8.0, and 10.0 by either adding 0.1 M HCl or 0.1 M NaOH. The equilibrium pH of supernatant was measured after shaking for 48 h at room temperature. We determine the pH_{pzc} as pH at the cross point between the plotted curve of equilibrium pH against initial pH and the line of pH (equilibrium) = pH (initial). Total specific surface area of the adsorbent was determined using the ethylene glycol monoethyl ether (EGME) method described by Cerato and Lutenegger (2002). Functional groups were determined by the Fourier-transform infrared (FT-IR) spectroscopy (FT/IR-620, JASCO). Spectra were collected with a spectrometer using potassium bromide (KBr) pellets and the opted wavenumber region was 400–4,000 cm^{-1}. Surface morphology and elemental distribution were identified by scanning electron microscopy (SEM) and energy-dispersive X-ray (EDX) instrument (SS-550 and Genesis 2000, Shimadzu). All the FT-IR, SEM, and EDX analyses were performed in the Analytical Center of Kyushu University.

2.3 Reagents

In the experiment, the fluoride solution was prepared using sodium fluoride (NaF) supplied from Wako Chemicals. Alfusone is the mixed powder of 2.5 % (w/w) lanthanum-alizarin complexone (mole ratio 1:1) chelate with potassium hydrogen phthalate and hexamethylenetetramine buffer. The alfusone was available from Dojindo Laboratories (Kumamoto, Japan) as the chromogenic reagent of the fluoride. A 1 % solution was prepared by dissolving the alfusone in distilled water in each analysis.

2.4 Determination of Actual and Apparent Fluoride Adsorption

Fluoride ion (F$^-$) concentration in the synthetic solutions (this ion exists as the form of HF with less than pH 3.16, pK_a of HF=3.16) was determined by the method reported by Okumura et al. (2003). We added 1 ml of the 1 % alfusone solution, 0.25 ml of filtrated solutions, 0.4 ml of buffer solution (CH$_3$COONa), and 2 ml of acetone into a test tube. The final volume was made up to 10 ml with distilled water. After a lapse of 60 min, 620-nm absorbance of the mixtures was measured by a spectrophotometer (Perkin-Elmer, Lambda 10). Metal-combined F$^-$ dissolved in acidic condition cannot be detected by the spectrophotometer. Since the adsorbed F$^-$ value can be evaluated as the difference between initial and final concentrations, the adsorption can be referred to as "apparent adsorption." As another adsorption measure, we defined "actual adsorption." It corresponds to the difference between the measured F$^-$ concentration and the concentration expected when acetylacetone is added as a demasking agent to detach F$^-$ from metal fluoride complexes.

2.5 Effect of pH on Fluoride Adsorption

The adsorption of fluoride on the feedstock and biochar was investigated at pH range of 2.0 to 10.0 using the method described by Oh et al. (2009). The pH of suspensions was adjusted by adding either 0.1 mol l^{-1} (M) HClO$_4$ or 0.1 M NaOH solution in a 10 ml polyethylene centrifuge tube. In the tube, we basically mixed 0.1 g of adsorbent samples with the solution of 2 ml of 0.5 M NaClO$_4$ and 2 ml of 5 mM NaF. The final volume of the mixture was made up to 10 ml with distilled water. In preliminary experiments, we identified that the pH was not changed after about 24 h. Thus, for stable equilibrium state of adsorption, we conducted the agitation of suspension in a shaker (Yamato, MK-200D) for 48 h in an air-conditioned room at 25 ± 1 °C. Thereafter, the suspensions were centrifuged at $2,100\times g$ for 15 min and filtered through a 0.22 μm Millipore filter. The solution samples obtained by the filtration were used for colorimetry analysis. The residual fluoride concentration in the filtrate was determined by using the spectrophotometer.

The adsorption of fluoride was calculated from the difference between the added fluoride and the final concentration in the solution.

3 Results and Discussion

3.1 Characteristics of Biochar

The physicochemical properties of raw feedstock and pyrolyzed biochar are shown in Tables 1 and 2. The OP and WS contain mainly oxides of calcium and potassium and oxides of aluminum, silica, and iron, respectively. These oxides would be hydroxylated to develop surface charge in aqueous medium and have a good capacity for fluoride adsorption. As the pyrolytic temperature increased from 400 to 700 °C, the pH increased from 11.6 to 12.3 for the OPB and from 6.4 to 6.8 for the WSB, respectively. This result was similar to that of Lehmann (2007), in which biochar was produced at a pH between 4.0 and 12.0, and the pH of fresh biochar increased with production temperature.

Surface areas of the OPB and WSB increased by 26.0–392.0 and 67.4–127.8 $m^2 g^{-1}$, respectively, compared with those of their feedstock. Ash contents of the OP and OPB were below 10 %, while those of WS and WSB ranged from 76 % to 90 %. Compared with the OPB, the higher ash content of the WSB can be attributed to the difference in carbon content between the WS and OP. This result was similar to that of Krull et al. (2009). Table 2 also shows the elemental contents of C, H, O, and N and their associated ratios, indicating the maturation degree of the biochar. As expected in the pyrolytic process, the C content of the biochar increased with increasing pyrolytic temperature, whereas the H and O contents decreased. The H/C and O/C ratios for the OPB and WSB tend to be the highest in low temperature and decreased with increasing pyrolytic temperature. According to Antal and Grønli (2003), this is a typical feedstock response in the pyrolytic process, i.e., the feedstock loses

surface functional OH^- groups due to dehydration at higher temperatures and also loses O and H atoms bound to C due to structural core degradation. In addition, Knicker et al. (2005) inferred the change in bonding arrangements from the H/C ratio of organic materials. These changes of the biochar surface may affect the fluoride adsorption.

3.2 Effect of pH on Fluoride Adsorption

The pH of aqueous solution is an important parameter controlling the adsorption process. The pH values may affect the surface charge of adsorbent, the degree of ionization, and the type of adsorbing element during adsorption process (Rahman and Islam 2009). Thus, we investigated the effect of pH on the adsorption of fluoride ions in the pH range of 2.0 to 10.0. Figures 1 and 2 show apparent and actual fluoride adsorption as a function of the pH for the OPB and WSB, respectively. No significant difference was found between apparent and actual fluoride adsorption (Fig. 1a and b). For OPB, the highest fluoride adsorption was found in between pH 2.0 and 3.3 and then the fluoride adsorption diminished drastically with increasing pH from 6.0 to 10.0. The fluoride adsorption was higher for OPB_{600} and OPB_{700} than for OPB_{400}. The OP adsorbed only a small amount of the fluoride in the whole pH range. On the other hand, apparent adsorption for the WS and WSB showed nearly 100 % in the pH range of 2.0 to 4.5, which adsorption quite differed from actual one. For the pH above 4.5, apparent adsorption decreased with increasing pH (Fig. 2a). The actual adsorption was greatly changed with pH (Fig. 2b). The maximum actual adsorption was 84.6 % for WS, 71.9 % for WSB_{400}, 57.7 % for WSB_{600}, and 76.4 % for WSB_{700}, respectively. From these values, the adsorption decreased sharply to 4.4 %, 16.1 %, 10.2 %, and 0.8 % at pH 10.0, respectively. For higher than pH 6.0, actual adsorption almost coincided with apparent adsorption. This demonstrates

Table 1 Principal chemical compositions of orange peel and water treatment sludge used as feedstock

(Unit: %) Feedstock	Al_2O_3	SiO_2	Fe_2O_3	CaO	K_2O	TiO_2	SO_3	P_2O_5	MnO	Total
Orange peel	–	–	1.0	66.1	28.4	–	2.8	1.7	–	100.0
Sludge	49.9	40.0	5.6	1.4	1.4	0.6	0.4	0.4	0.3	100.0

Table 2 Physicochemical properties of the each biochar prepared under different pyrolytic temperatures

Feedstock	Pyrolysis temperature (°C)	pH (1:10)	pH$_{pzc}$ (1:10)	SSA (m^2 g^{-1})	Element content (%)				H/C ratio	O/C ratio	Ash (%)
					C	H	N	O			
Orange peel	0	4.1	4.1	24.0	41.9	6.4	1.0	47.9	1.8	0.9	2.9
	400	11.6	7.4	428.0	68.4	4.8	2.0	19.8	0.8	0.2	5.0
	600	12.1	9.8	137.1	74.7	2.1	1.7	13.4	0.3	0.1	8.1
	700	12.3	10.0	110.2	74.8	1.6	1.7	13.4	0.3	0.1	8.5
Sludge	0	5.7	5.7	93.5	6.6	1.8	0.3	15.3	3.2	1.7	76.0
	400	6.4	6.2	126.4	8.5	1.0	0.3	6.4	1.4	0.6	83.7
	600	6.6	6.5	114.4	8.4	0.6	0.2	2.0	0.9	0.2	88.8
	700	6.8	6.2	135.2	8.1	0.5	0.2	0.6	0.7	0.1	90.7

SSA Specific surface area, *H/C* atomic ratio of hydrogen to carbon, *O/C* atomic ratio of oxygen to carbon

that the fluoride separated by acetylacetone from metal fluoride complexes exists with conformation of HF or F$^-$. In the actual adsorption for the WS and WSB, the maximum values appeared in the pH range of 5.1 to 6.2

(Fig. 2b). This result was similar to those in the fluoride adsorption experiments in literatures, i.e., at pH 5.5 for refractory grade bauxite (Mohapatra et al. 2004), pH 6.0 for montmorillonite (Tor 2006), and pH 5.5 for
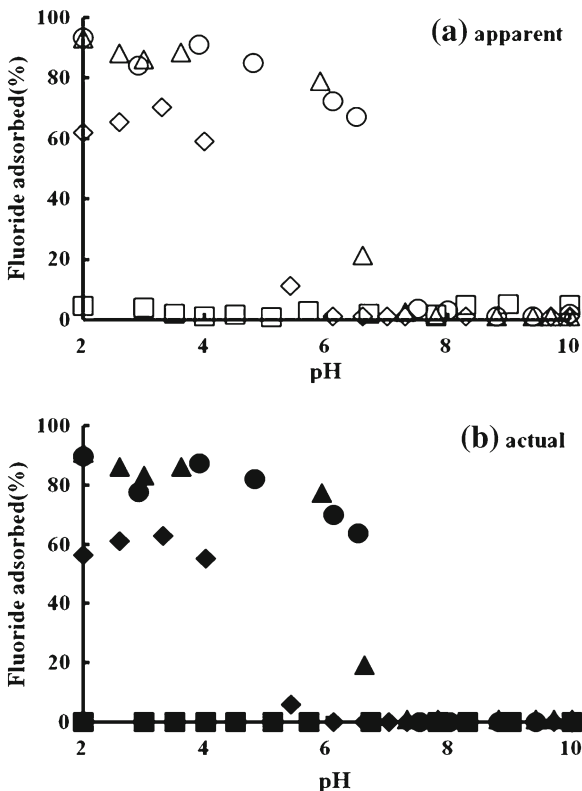

Fig. 1 Apparent (*open*) and actual (*solid*) fluoride adsorption as a function of pH. (■ and □, OP; ◆ and ◇, OPB$_{400}$; ▲ and △, OPB$_{600}$; ● and ○, OPB$_{700}$). Conditions: Adsorbent 0.1 g, fluoride concentration (NaF) 1 mM, time 24 h, NaClO$_4$ 0.1 M, final volume 10 ml
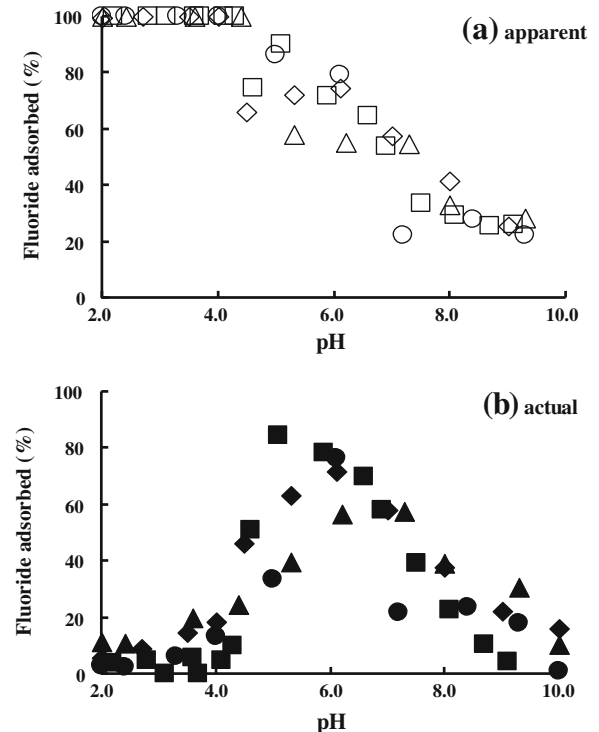

Fig. 2 Apparent (*open*) and actual (*solid*) fluoride adsorption as a function of pH. (■ and □, WS; ◆ and ◇, WS$_{400}$; ▲ and △, WS$_{600}$; ● and ○, WS$_{700}$). Conditions : Adsorbent 0.1 g, fluoride concentration (NaF) 1 mM, time 24 h, NaClO$_4$ 0.1 M, final volume 10 ml

manganese-dioxide-coated activated alumina (Tripathy and Raichur 2008).

Unlike the OP and OPB, the fluoride adsorption for WS and WSB depicted significantly different behaviors between apparent and actual adsorption (Fig. 2a and b). These differences would occur in acidic range depending on the fluoride conformation dissolved in the solution. In the range of pH 2.0 to 4.5, the fluoride can be exchanged by hydroxyl group (-OH) combined with metal ions such as aluminum and iron on the WS and WSB surfaces. The metal fluoride complexes can be ultimately detached from the WS and WSB surfaces into an aqueous phase. As shown in Table 1, the WS contains oxides of aluminum and iron to a large extent. These oxides on the WS and WSB surfaces would be hydroxylated to develop surface charge in the aqueous solution (Oh and Chikushi 2010). This suggests that most of the fluoride may exist as soluble metal fluoride such as fluoro-aluminates complexes (AlF_i^{3-i}) in the acidic condition. The effect of pH on the fluoride adsorption for the WS and WSB can also be explained on the basis of the point of zero charge (pH_{pzc}). When solution pH is below the pH_{pzc}, positively charged surfaces can adsorb anions such as fluoride due to the electrostatic attraction. For pH above the pH_{pzc}, the reduction of fluoride adsorption can be attributed to the electrostatic repulsion from the negatively charged surfaces or to the competition between hydroxide and fluoride anions.

From these results, reasonable reaction mechanisms on the biochar surface are described in acidic condition as:

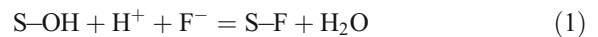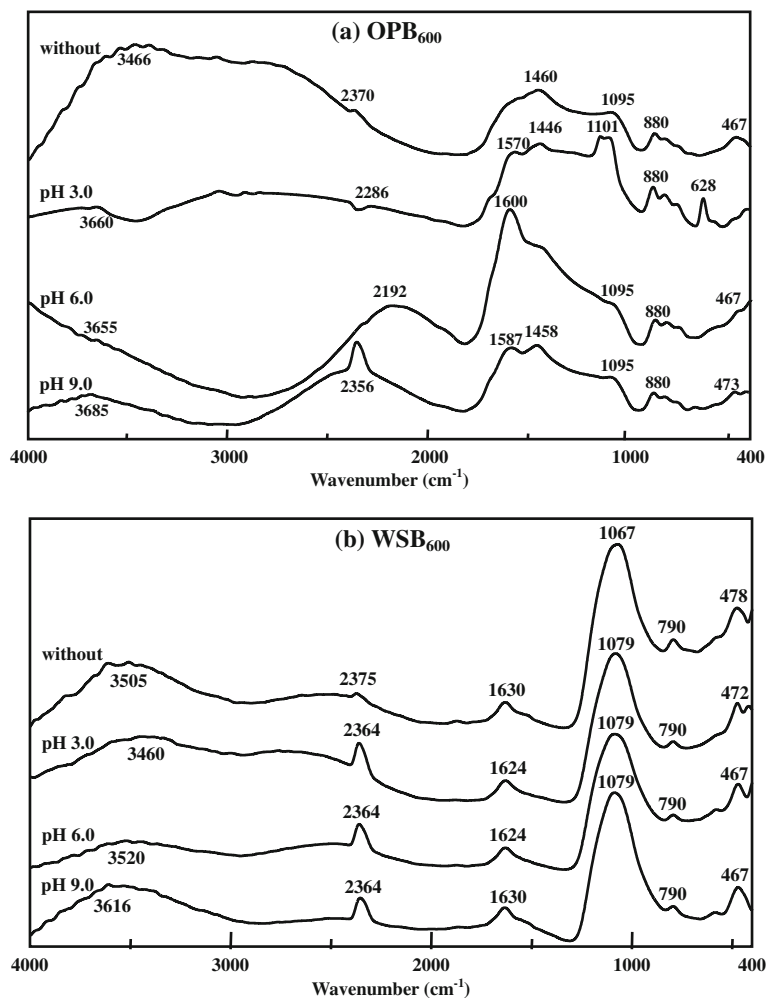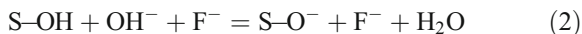$$S\text{–}OH + H^+ + F^- = S\text{–}F + H_2O \tag{1}$$

Fig. 3 Fourier-transform infrared (FT-IR) spectroscopy changes of OPB (a) and WSB (b) produced at 600 °C without and with fluoride adsorption at pH 3.0, 6.0, and 9.0

and in basic condition as:

$$S–OH + OH^- + F^- = S–O^- + F^- + H_2O \qquad (2)$$

where S represents the surface of biochar.

It can be deduced that the biochar surface had more positive charges (mainly $S–OH_2^+$ groups) in acidic condition and was able to adsorb easily the fluoride ions, indicating a high adsorption rate. In basic condition, the biochar surface had more negative charges (mainly $S–O^-$ groups) and tended to inhibit the adsorption of fluoride ions to the biochar surface. In short, the adsorption of fluoride on the biochar is strongly pH-dependent.

3.3 FT-IR Analysis

The fluoride adsorption by the biochar may be affected strongly by the functional groups and by the carbon behavior on the biochar surfaces. The FT-IR spectra were, therefore, investigated to analyzed major functional groups present in the OPB and WSB. Figure 3

shows the results of the FT-IR spectra for OPB_{600} and WSB_{600} without (no F^- in solution) and with adsorption conditions at pH 3.0, 6.0, and 9.0. In the spectra of the OPB_{600}, various bands are observed on C=O $(1,570–1,600 \text{ cm}^{-1})$, C–H $(1,450–1,460 \text{ cm}^{-1})$, and CH_2 (880 cm^{-1}). In the OPB_{600} without the adsorption condition, the strong and broad –OH peak over 3,400–3,680 cm^{-1} was revealed, and the intensity of the peak decreased with the adsorption conditions at pH 3.0 and 6.0 (Fig. 3a). The spectra of WSB_{600} were different from those of OPB_{600} in intensity and shape. This might be caused by the difference of constituents between two types of the raw feedstock. In the WSB_{600}, the band between 400 and 800 cm^{-1} can be attributed to the superposition of the specific vibrations of various oxides. The occurrence of peak around 1,630 cm^{-1} may be due to the vibrating property of C=C. With the adsorption conditions, the band observed at around 2,364 cm^{-1} becomes strong and sharp. This suggests that the appearance of the 2,364 cm^{-1} peak may be due to the fluoride adsorption
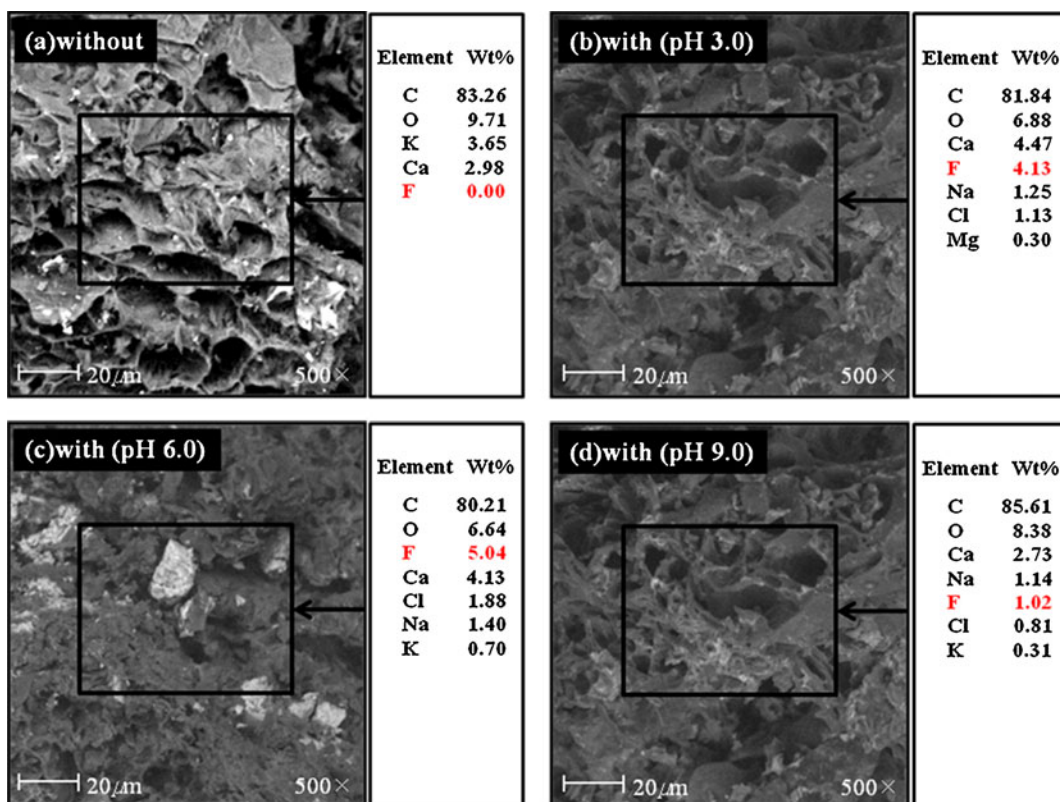

Fig. 4 Scanning electron micrographs(SEM) image and associated energy dispersive X-ray (EDX) quantification changes of OPB produced at 600 °C without (**a**) and with fluoride adsorption at pH 3.0 (**b**), 6.0 (**c**), and 9.0 (**d**)

on the corresponding carbon dioxide. The analysis of FT-IR at different pH conditions suggested that OH^- groups may affect the adsorption of fluoride because OH^- and F^- anions have approximately same size, which can be isomorphously replaced each other (Ayoob et al. 2008). Thus, the reduction of fluoride adsorption observed under basic conditions can be explained by the competition between hydroxide and fluoride anions.

3.4 SEM and EDX Analyses

To understand the properties of fluoride adsorption at the different pH conditions, the SEM image and EDX quantification of the OPB_{600} and WSB_{600} were performed without and with adsorption conditions at the pH 3.0, 6.0, and 9.0. The results are shown in Figs. 4 and 5, respectively. The OPB_{600} and WSB_{600} were composed of very coarse and heterogeneous surfaces, having significantly irregular forms and sizes of the particles, especially the OPB_{600} was imaged with

many hollow channels of around 10–20 μm in diameters. These structures of the OPB and WSB are likely to provide a high internal surface area and adsorption ability as an absorbent for the fluoride. Elemental analysis by the EDX demonstrated the presence of fluoride dissolved in the sample solutions at the different pH conditions. Comparison of the elemental content in Figs. 4 and 5 showed that fluorine content was higher at pH 6.0 than at pH 3.0 and pH 9.0. This result coincided with those in Figs. 1 and 2. That is, the relatively low F content at pH 3.0 implies that the fluoride combined with metal ions such as aluminum and iron in the WSB could be detached from the surface and these fluoride complexes could be kept in the aqueous solution (Fig. 5). According to Sujana and Anand (2010), the SEM–EDX analysis revealed the fluoride adsorption on adsorbent surface and indicated that both iron and aluminum contributes to the fluoride adsorption. Kumar et al. (2011) also reported from the EDX analysis that elemental constituents interacts with fluoride adsorbent.
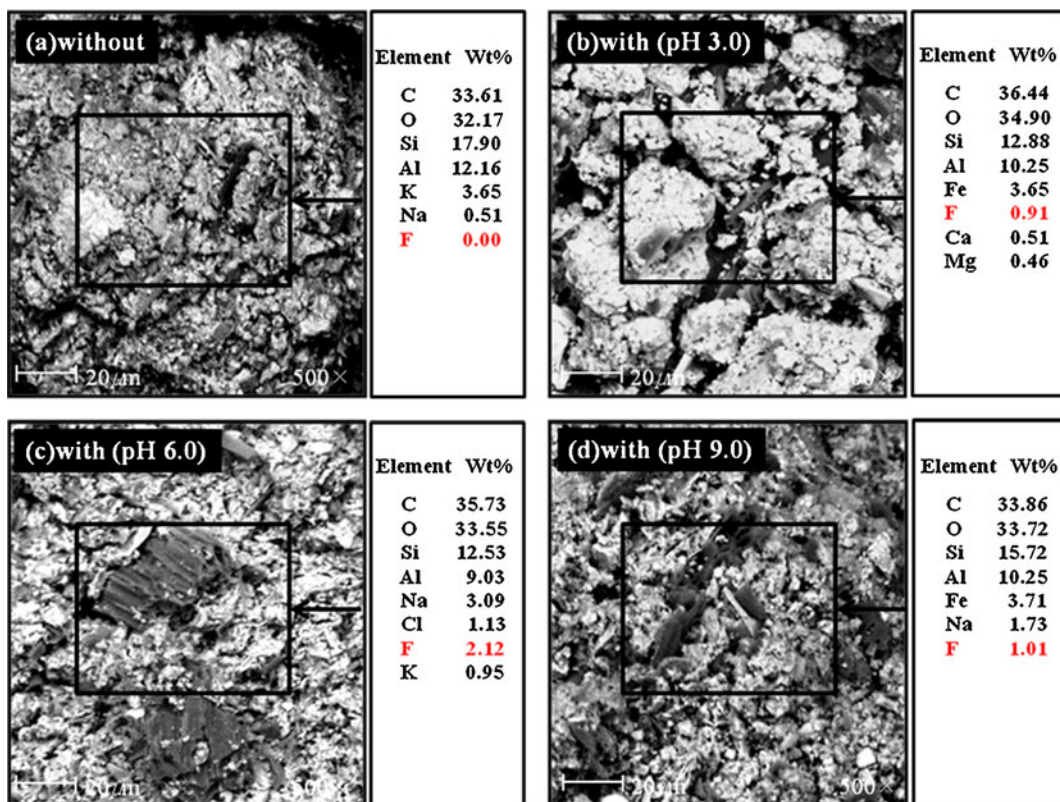

Fig. 5 Scanning electron micrographs(SEM) image and associated energy dispersive X-ray (EDX) quantification changes of WSB produced at 600 °C without (a) and with fluoride adsorption at pH 3.0 (b), 6.0 (c), and 9.0 (d)

4 Conclusions

Fluoride adsorption is strongly dependent on pH conditions. This study reveals that the fluoride ion in acidic conditions can be efficiently adsorbed by biochar produced from OP and WS. The reduction of fluoride adsorption in the basic condition would occur because of the competition between hydroxide and fluoride anions. In the WSB containing Al as major components, the difference of apparent and actual fluoride adsorption would occur because of the fluoride conformations dissolved in the solution. That is, considerable amount of fluoride leached from the functional groups in WSB with the adsorption condition and existed as soluble fluoro-aluminate complexes in low pH solutions. This reaction was also identified by comparison of elemental contents measured by EDX at different pH conditions. In conclusion, the use of biochar derived from OP and WS are found to be an environmental and cost-effective adsorbent for fluoride adsorption and hence can be considered as a promising alternative for defluoridation in acidic aqueous phase.

References

Antal, M. J., & Grønli, M., Jr. (2003). The art, science, and technology of charcoal production. *Industrial and Engineering Chemistry Research, 42*(8), 1619–1640.

Ayoob, S., & Gupta, A. K. (2006). Fluoride in drinking water: a review on the status and stress effects. *Environmental Science and Technology, 36*(6), 433–487.

Ayoob, S., Gupta, A. K., Bhakat, P. B., & Bhat, V. T. (2008). Investigations on the kinetics and mechanisms of sorptive removal of fluoride from water using alumina cement granules. *Chemical Engineering Journal, 140*(1–3), 6–14.

Cerato, A. B., & Lutenegger, A. J. (2002). Determination of surface area of fine-grained soils by the ethylene glycol mono-ethyl ether (EGME) method. *Geotechnical Testing Journal, 25*(3), 1–7.

Chae, G. T., Koh, D. C., & Choi, B. Y. (2008). The origin and geochemical behavior of fluoride in bedrock groundwater: a case study in Samseung area (Boeun, Chungbuk). *Journal of Engineering Geology, 18*(4), 555–566 (in Korean).

Chen, B., & Chen, Z. (2009). Sorption of naphthalene and 1-naphthol by biochars of orange peels with different pyrolytic temperatures. *Chemosphere, 76*(1), 127–133.

Groves, B. (2001). *Fluoride: Drinking ourselves to death.* Dublin: Newleaf.

Harrison, P. T. C. (2005). Fluoride in water: a UK perspective. *Journal of Fluorine Chemistry, 126*(11/12), 1448–1456.

Ishii, T., & Suckling, G. (1991). The severity of dental fluorosis in children exposed to water with a high fluoride content for various periods of time. *Journal of Dental Research, 70* (6), 952–956.

Knicker, H., Totsche, K. U., Almendros, G., & Gonzalez-Vila, F. J. (2005). Condensation degree of burnt peat and plant residues and the reliability of solid-state VACP MAS ^{13}C NMR spectra obtained from pyrogenic humic material. *Organic Geochemistry, 36*(10), 1359–1377.

Krull, E., Baldock, J., Skjemstad, J., & Smernik, N. (2009). Characteristics of biochar: Organo-chemical properties. In J. Lehmann & S. Joseph (Eds.), *Biochar for environmental management: Science and technology.* London: Earthscan.

Kumar, E., Bhatnagar, A., Kumar, U., & Sillanpää, M. (2011). Defluoridation from aqueous solutions by nano-alumina: characterization and sorption studies. *Journal of Hazardous Materials, 186*(2–3), 1042–1049.

Lehmann, J. (2007). Bio-energy in the black. *Frontier in Ecology and the Environment, 5*(7), 381–387.

Lehmann, J., & Joseph, S. (2009). In J. Lehmann & S. Joseph (Eds.), *Biochar for environmental management: Science and technology.* London: Earthscan.

Meenakshi, S., & Maheshwari, R. C. (2006). Fluoride in drinking water and its removal. *Journal of Hazardous Materials, B137*(1), 456–463.

Mohapatra, D., Mishra, D., Mishra, S. P., Roy-Chaudhury, G., & Das, R. P. (2004). Use of oxide minerals to abate fluoride from water. *Journal of Colloid and Interface Science, 275* (2), 355–359.

Oh, T. K., & Chikushi, J. (2010). Fluoride adsorption on water treatment sludge processed by polyaluminium chloride. *Journal of Food Agriculture and Environment, 8*(1), 358–362.

Oh, T. K., Chikushi, J., & Saeki, K. (2009). The adsorption of hydrogen fluoride and fluoride ion on a water treatment sludge. *Journal of the Faculty of Agriculture Kyushu University, 54*(1), 205–208.

Oh, T. K., Choi, B. S., Shinogi, Y., & Chikushi, J. (2012). Characterization of biochar derived from three types of biomass. *Journal of the Faculty of Agriculture Kyushu University, 57*(1), 61–66.

Okumura, M., Yoshimura, T., Fujinaga, K., & Seike, Y. (2003). Direct spectrophotometric determination of traces of fluoride in rain water. *The Japan Society for Analytical Chemistry, 52* (6), 485–488 (in Japanese).

Rahman, M. S., & Islam, M. R. (2009). Effects of pH on isotherms modeling for Cu(II) ions adsorption using maple wood sawdust. *Chemical Engineering Journal, 149*, 273–280.

Rao, C. R. N., & Karthikeyan, J. (2011). Removal of fluoride from water by adsorption onto lanthanum oxide. *Water, Air, and Soil Pollution*. doi:10.1007/s11270-011-0928-0.

Sujana, M. G., & Anand, S. (2010). Iron and aluminium based mixed hydroxides: a novel sorbent for fluoride removal from aqueous solutions. *Applied Surface Science, 256* (26), 6956–6962.

Tchomgui-Kamga, E., Ngameni, E., & Darchen, A. (2010). Evaluation of removal efficiency of fluoride from aqueous solution using new charcoals that contain calcium compounds. *Journal of Colloid and Interface Science, 346*(2), 494–499.

Tor, A. (2006). Removal of fluoride from an aqueous solution by using montmorillonite. *Desalination, 201*(1–3), 267–276.

Tripathy, S. S., & Raichur, A. M. (2008). Abatement of fluoride from water using manganese dioxide-coated activated alumina. *Journal of Hazardous Materials, 153*(3), 1043–1051.

World Health Organization (1994). *Fluorides and oral health*. Technical Report Series No. 846. World Health Organisation: Geneva.

World Health Organization (2006). *Guidelines for drinking-water quality*, 3rd edition, 1st addendum to vol. 1. WHO.

Zheng, W., Guo, M., Chow, T., Bennet, D. N., & Rajagopalan, N. (2010). Sorption properties of greenwaste biochar for two triazine pesticides. *Journal of Hazardous Materials, 181*(1–3), 121–126.